Bioorganic & Medicinal Chemistry Letters 21 (2011) 2869–2872

Contents lists available at ScienceDirect

Bioorganic & Medicinal Chemistry Letters

journal homepage: www.elsevier.com/locate/bmcl

The Synthesis and evaluation of a novel class of (*E*)-3-(1-cyclohexyl-1*H*-pyrazol-3-yl)-2-methylacrylic acid Hepatitis C virus polymerase NS5B inhibitors

Scott W. Martin [a,*], Peter Glunz [c,*], Brett R. Beno [b], Carl Bergstrom [a], Jeffrey L. Romine [a], E. Scott Priestley [c], Makenzie Newman [c], Min Gao [d], Susan Roberts [d], Karen Rigat [d], Robert Fridell [d], Dike Qiu [d], Galina Knobloh [d], Ying-Kai Wang [d]

[a] Department of Chemistry, Bristol-Myers Squibb Research and Development, 5 Research Parkway Wallingford, CT 06492, United States
[b] Computer-Assisted Drug Design Department, Applied Biotechnology, Bristol-Myers Squibb Research and Development, 5 Research Parkway Wallingford, CT 06492, United States
[c] Department of Chemistry, Bristol-Myers Squibb Research and Development, 311 Penington-Rocky Hill Rd. Hopewell, NJ 08534, United States
[d] Department of Virology, Bristol-Myers Squibb Research and Development, 5 Research Parkway Wallingford, CT 06492, United States

ARTICLE INFO

Article history:
Received 3 February 2011
Revised 18 March 2011
Accepted 22 March 2011
Available online 30 March 2011

Keywords:
Hepatitis
Polymerase
NS5B
Inhibitors
Pyrazoles

ABSTRACT

Herein we report the identification and evaluation of a novel series of (*E*)-3-(1-cyclohexyl-1*H*-pyrazol-3-yl)-2-methylacrylic acid derivatives identified from a deannulation study performed on the reported benzimidazole NS5B inhibitor, **1**. This resulted in the identification of (*E*)-3-(2-(4-((4′-cyano-4-(4-hydroxypiperidine-1-carbonyl)biphenyl-2-yl)methoxy)phenyl)-1-cyclohexyl-1*H*-imidazol-4-yl)-2-methylacrylic acid (**11**) as a potent inhibitor of NS5B. Potential pathways for the further optimization of this series are suggested.

Hepatitis C virus (HCV) is estimated to have chronically infected 160 million people worldwide with 5.3 million cases reported in the United States.[1] Infection with HCV can result in the development of a chronic condition that frequently progresses to cirrhosis and hepatocellular carcinoma.[2,3] The current optimal treatment involves extended administration with PEG-interferon-α and ribavirin,[4,5] although a number of advanced clinical studies employing direct acting antivirals (DAA) may be on the verge of changing current optimal thearapy.[5b,c] The current regime suffers from limited efficacy against 1a and 1b HCV genotypes and is associated with an array of severe side effects. This latter issue leads to treatment discontinuation in a significant proportion of patients.[5a,6] Correspondingly, there exists a clear and urgent medical need for improved therapeutic agents. HCV non-structural protein 5B (NS5B), an RNA-dependent RNA-polymerase (RdRp) has long been considered an attractive target for drug discovery due to its essential role in viral replication.[5a,7] In addition to a number of reported active site inhibitors, multiple allosteric inhibitors have been identified that act at four distinct binding sites,[5b,8][Pockets 1–4]. Analogs of compound **1**[9] have been reported to bind in pocket I of NS5B,[8,10,11] a site that has been clinically validated.[5b,12] Correspondingly, we became interested in evaluating novel derivatives of **1**, and examined a number of possible structural modifications to this compound.

One of our more productive approaches explored a deannulation strategy in which we excised a single carbon atom from the benzimidazole to generate the acrylate **2**, as shown in Figure 1. This compound displayed an approximate three-fold reduction in potency. Replacement of the imidazole heterocycle in **2** with an isomeric pyrazole, as shown in analog **3**, was associated with a further loss of activity. Surprisingly however, the positional pyrazole isomer **4** was essentially equipotent with the original lead **1**, and led us to evaluate the series of pyrazol-3-yl-2-methylacrylic acids shown in Table 1.

Scheme 1 outlines the synthetic route used to access pyrazoles **4** through **14**. Compounds **1**,[9] **2** and **3**[13] were prepared as previously reported.

Diketoester **15**[15] was condensed with cyclohexyl hydrazine in refluxing ethanol to generate the pyrazole **16**. Reduction with lithium aluminum hydride gave an alcohol which, upon subsequent oxidation with manganese(IV)oxide, provided an aldehyde that could be reacted with the in situ-generated Wittig reagent derived from 1-[(ethoxycarbonyl)ethyl]triphenylphosphonium bromide. The resultant methacrylate **18** was debenzylated upon exposure to boron trichloride, and subsequent alkylation with the benzyl bromide **20**[9b] gave key intermediate **21**. Compound **21** allowed

* Corresponding authors.
E-mail address: scott.martin@bms.com (S.W. Martin).

0960-894X/$ - see front matter © 2011 Elsevier Ltd. All rights reserved.
doi:10.1016/j.bmcl.2011.03.086

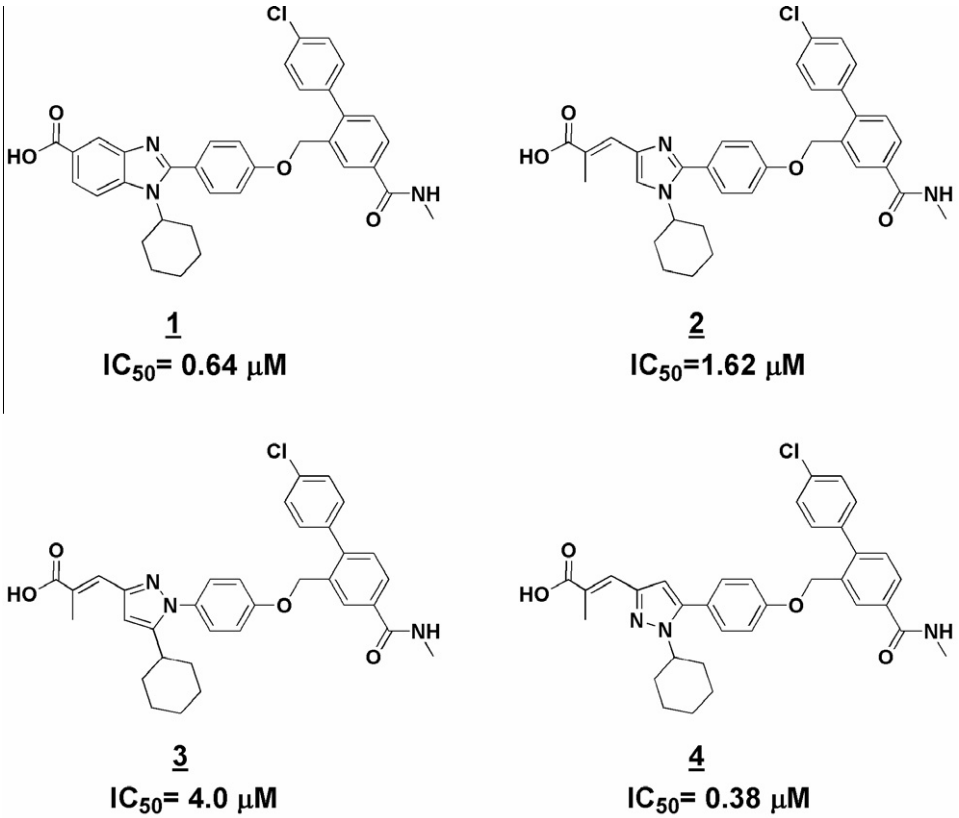

Figure 1. Literature disclosed NS5B allosteric inhibitor **1**[9], and related deannulated analogs **2**, **3** and **4** displaying NS5B inhibitory activity.[13]

Table 1
Inhibition of HCV NS5B genotype 1b enzyme;[13] structures corresponding to Figure 1 and Figure 4

Compd	Ar	R^1	R^2	IC_{50}[a] (μM)
1[b]	4-Cl-phenyl	CH_3NH		0.64 (±0.15)
2[b]	4-Cl-phenyl	CH_3NH		1.62 (±0.26)
3[b]	4-Cl-phenyl	CH_3NH		4.03 (n = 1)
4	4-Cl-phenyl	CH_3NH	H	0.38 (n = 1)
5	4-Cl-phenyl	$(CH_3)_2N$	H	0.46 (±0.31)
6	4-Cl-phenyl	4-OH-piperidine	H	0.44 (±0.12)
7	4-Cl-phenyl	4-OH-piperidine	Br	0.65 (±0.14)
8	4-Cl-phenyl	$NHCH_2CH_2$ OH	H	1.03 (±0.13)
9	4-CN-phenyl	CH_3NH	H	0.79 (±0.11)
10	4-CN-phenyl	$(CH_3)_2N$	H	0.82 (±0.60)
11	4-CN-phenyl	4-OH-piperidine	H	0.34 (±0.06)
12	5-Acetyl-thiophen-2-yl	CH_3NH	H	2.29 (±0.03)
13	5-Acetyl-thiophen-2-yl	$(CH_3)_2N$	H	2.7 (±1.2)
14	5-Acetyl-thiophen-2-yl	Morpholine	H	5.2 (±1.2)

[a] Values are means of a minimum of two test occasions run in duplicate, standard deviation is given in parentheses, values with n = 1 are single test occasions run in duplicate.
[b] Structures corresponding to Figure 1.

for diversification at two vectors: the aryl side chain through Suzuki coupling, and amide formation to **23** upon selectively unmasking the *t*-butyl carboxylate. Hydrolysis of the acrylate ester led to compounds **4–6** and **8–14** as shown in Table 1, where R^2 = H. Functionalization at R^2 was achieved through the bromo pyrazole **17** obtained upon bromination of **16** with bromine in acetic acid. Bromide **17** was further transformed into acrylate **19** via chemistry analogous to that used in the preparation of **18**. A more convergent approach was employed in the synthesis of compound **7** (Scheme 1). Debenzylation of **19** followed by Mitsunobu alkylation with the biaryl derivative **22**[16] directly gave **24** and thus eliminated possible chemoselectivity concerns related to using a dibromide in a subsequent Suzuki reaction (e.g., **21** to **23**). Target compound **7** was obtained from **24** after ester hydrolysis.

As stated above, we evaluated a number of isomeric diazole cores in our deannulation approach to the synthesis of novel analogs of compound **1**. Of these, pyrazole **4** was found to be approximately four-fold more active than analog **2**, and ten-fold more potent than its isomeric counterpart **3** (Table 1). These observations may be accounted for based on variations in the binding interactions between each of the ligands' carboxylate moieties and Arg503 of NS5B, as suggested by molecular modeling studies. For example, the superposition of analogs **2, 3** and **4** with compound **B**, as shown in Figure 2, (*from published NS5B/Compound **B** co-crystal structure*[17]) demonstrates that as the distances between the carboxylate oxygen atoms and the Arg503 guanidine nitrogen atoms increase, potency decreases.

We concluded that differences in the bond lengths and angles in the pyrazole and imidazole rings translate to different positioning of the carboxylate moieties relative to the cyclohexyl group that serves to anchor these compounds in the polymerase, and thus impact the strength of the interactions between the acid functionalities of the ligand and Arg503. An obvious alternative explanation is that the less potent diazoles described here could be expected to experience allylic strain[25] when adopting the probable bioactive conformation, see Figure 3.

Pursuing our initial rationale for the observed enhanced activity of analog **4**, we prepared the series of derivatives shown in Table 1, based on the generic structure depicted in Figure 4.

Significant structure-activity relationship (SAR) of the biaryl side chain of the benzimidazole reference compound **1** has been established in a previous report.[9b] From the above Table 1 it can be seen that the combination of an *N*-methyl, *N*,*N*-dimethyl, or piperidin-4-ol amide appended to either a 4-cyano or 4-chloro biaryl as shown in analogs **1–7** and **9**–**11**, respectively, generally

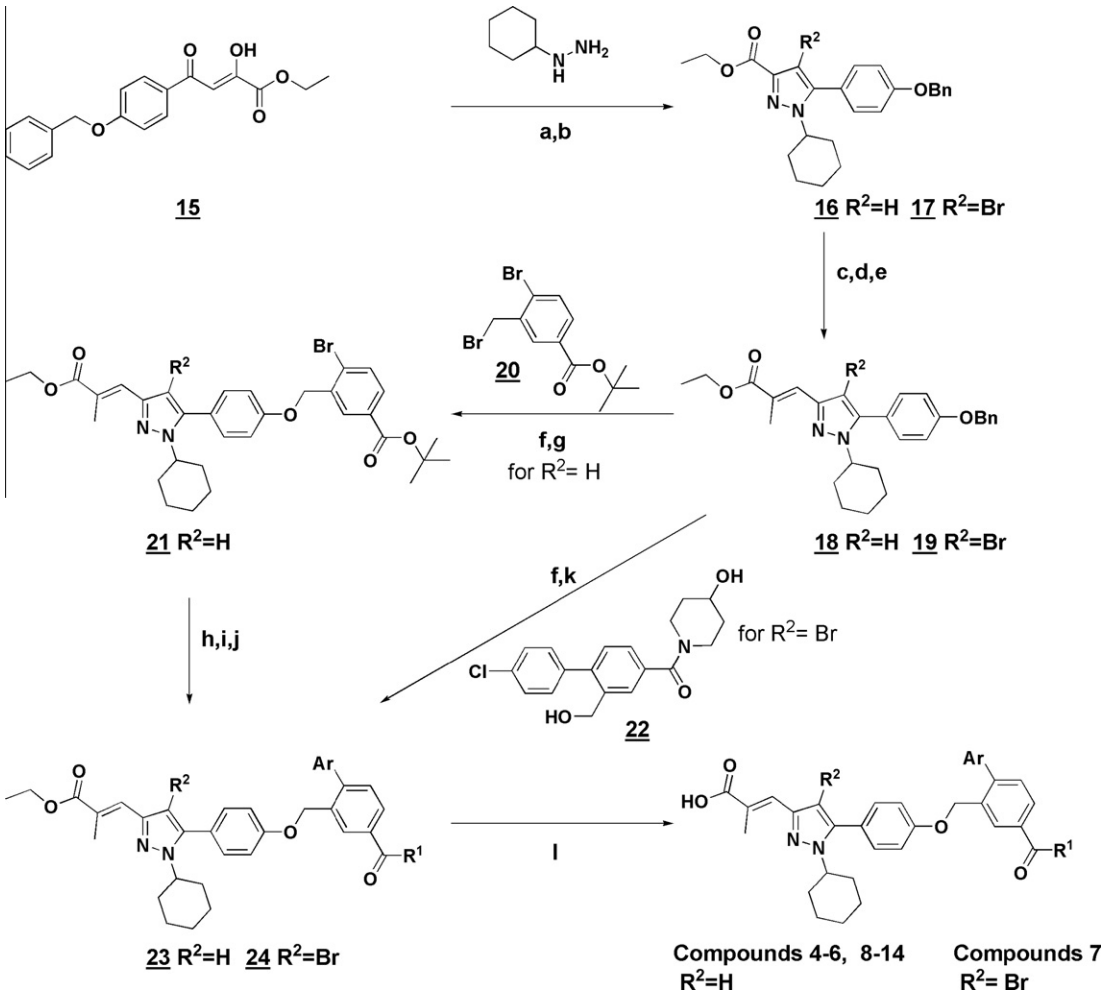

Scheme 1. Reagents and conditions: (a) ethanol reflux; (b) for R^2 = Br, Br_2, AcOH, 0 °C to rt; (c) $LiAlH_4$, THF, 0 °C to rt; (d) MnO_2, DME, reflux; (e) [1-(ethoxycarbonyl)ethyl]triphenylphosphonium bromide, *n*-BuLi, THF, 0 °C to rt; (f) BCl_3, CH_2Cl_2, −40 °C; (g) Cs_2CO_3, DMF, rt; (h) Ar-$B(OH)_2$, $(Ph_3P)_4Pd$, THF, satd aqueous $NaHCO_3$, reflux 18 h, or Ar-$B(OH)_2$, $(Ph_3P)_4Pd$, 1,4-dioxane, satd aqueous $NaHCO_3$, microwave 120 °C, 10 min. (i) TFA, CH_2Cl_2, rt; (j) TBTU, DMF, amine, rt; (k) DIAD, Ph_3P, THF, 0 °C to rt; (l) NaOH, THF, 60 °C.

results in sub-micromolar potency against NS5B. This SAR parallels findings reported in the series typified by compound **1**, where introduction of a small electron withdrawing group and inclusion of a carbonyl moiety in the 4-position of the biaryl side chain enhanced intrinsic potency and whole cell activity while modulating protein binding and cellular toxicity.[9b] Compound **11** displayed similar potency to the parent benzimidazole **1** in both the enzyme NS5B assay,[13] and in a subsequent genotype **1b** replicon assay[14] (compound **11** EC_{50} = 0.4 ± 0.2 μM vs compound **1** EC_{50} of 0.3 μM *n* = 1). Moreover, compound **11** demonstrated a ten-fold loss in activity (EC_{50} = 4.0 μM) against the mutant P495A replicon system, strongly supporting the assumption that this analog binds in pocket 1. Compound **11** was determined to be relatively non-toxic (CC_{50} = 25 μM) and had a therapeutic index of >60. In addition, the closely related analog **5** (replicon EC_{50} = 1.9 ± 1.3 μM) was shown to have good bioavailability in rat when dosed orally at 2 mg/Kg, (F = 69%, $T_{1/2}$ = 1.3 ± 0.7 h), thus demonstrating the potential of pyrazol-3-yl-2-methylacrylic acids to possess favorable absorption properties.

Compounds **12–14**, in which the distal phenyl moiety of the biphenyl group is replaced with a thiophene isostere, and compound **8**, that incorporates an extended 2-hydroxyethyl functionality in the amide group, generally displayed a moderate loss of activity.

As can be seen with compound **7**, substitution at position C4 (R^2 = Br) afforded a compound with comparable activity in both

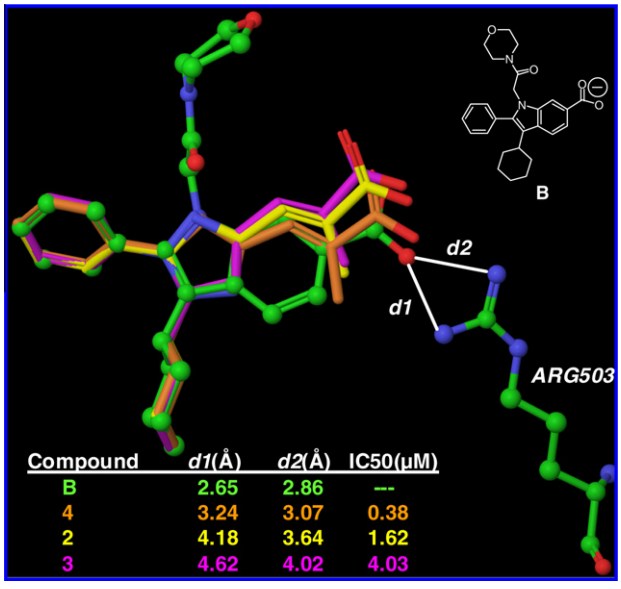

Figure 2. Interaction of core carboxylate moieties with NS5B ARG503. Geometries of truncated core molecules **2**–**4** optimized with DFT at the B3LYP/6–31G** level using Q-Chem.[19–24] See Ref. 18.

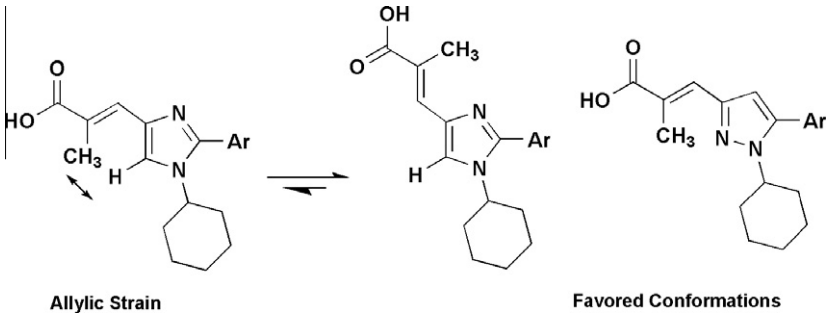

Figure 3. Preferred conformations of pyrazole and imidazole inhibitor classes.

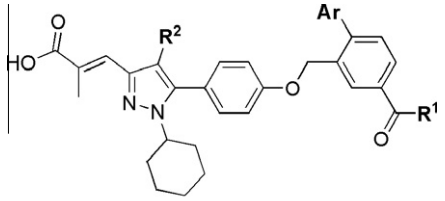

4-14

Figure 4. Pyrazole heterocycle structures associated with Table 1 (unless otherwise noted).

the enzyme (IC_{50} = 0.65 ± 0.14 μM) and replicon (EC_{50} = 0.7 ± 0.4 μM) assays. This bromine substituent provides a chemical handle to exploit an additional vector for further potency and pharmacokinetic optimization. Related studies at the N1 position of indole chemotype **B** shown in Figure 2, resulted in significant modulation of both physicochemical properties and cell based efficacy.[26] A future disclosure will detail our research investigating this region.

In conclusion, we have described a novel series of (*E*)-3-(1-cyclohexyl-1*H*-pyrazol-3-yl)-2-methylacrylic acid NS5B inhibitors identified from a deannulation study performed on the known benzimidazole inhibitor **1**. The relative potencies of a series of isomeric 2-methylacrylate appended heterocycles could be rationalized with regard to molecular modeling predictions of variations in the strengths of the interactions of the ligands' carboxyl moieties with Arg503 of NS5B. Subsequent elucidation of an initial structure–activity relationship of the pyrazole **4** identified compounds with potencies in both enzyme and replicon assays, comparable to the parent chemotype **1**. Data from resistance studies strongly suggested these compounds bind in Pocket 1. Finally, in analog **7**, we have identified paths for the further optimization of this compound class.

Acknowledgments

The corresponding authors acknowledge Dr. Carl Bergstrom for his significant help in reviewing this manuscript.

Supplementary data

Supplementary data associated with this article can be found, in the online version, at doi:10.1016/j.bmcl.2011.03.086.

References and notes

1. Lavanchy, D. *Clin. Microbiol. Infect.* **2011**, *17*, 107.
2. Di Bisceglie, A. M.; Order, S. E.; Klein, J. L.; Waggoner, J. G.; Sjogren, M. H.; Kuo, G.; Houghton, M.; Choo, Q.-L.; Hoofnagle, J. H. *Am. J. Gastroenterol.* **1991**, *86*, 335.
3. Raimondi, S.; Bruno, S.; Mondelli, M. U.; Maisonneuve, P. *J. Hepatol.* **2009**, *50*, 1142.
4. Ferenci, P.; Fried, M. W.; Shiffman, M. L.; Smith, C. I.; Marinos, G.; Goncales, F. L., Jr.; Haussinger, D.; Diago, M.; Carosi, G.; Dhumeau, D.; Craxi, A.; Chaneac, M.; Reddy, K. R. *J. Hepatol.* **2005**, *43*, 425.
5. (a) Beaulieu, P. L. *Expert Opin. Ther. Pat.* **2009**, *19*, 145; (b) Watkins, W. J.; Ray, A. S.; Chong, L. S. *Curr. Opin. Drug Discovery Dev.* **2010**, *13*, 441; (c) Vermehren, J.; Sarrazin, C. *Clin. Microbiol. Infect.* **2011**, *17*, 122.
6. Sarbah, S. A.; Younossi, Z. M. *J. Clin. Gastroenterol.* **2000**, *30*, 125.
7. Lindenbach, B. D.; Rice, C. M. *Nature* **2005**, *436*, 933.
8. Talele, T. T. *Curr. Bioact. Compd.* **2008**, *4*, 86.
9. (a) Hashimoto, H.; Mizutani, K.; Yoshida, A. U.S. Patent 6770,666 B2, 2004.; (b) Suzuki, T.; Hirashima, S.; Ishida, T.; Noji, S.; Yata, S.; Ando, I.; Komatsu, M.; Ikeda, S.; Hashimoto, H. *J. Med. Chem.* **2006**, *49*, 4721.
10. Beaulieu, P. L. *Curr. Opin. Drug Discovery Dev.* **2006**, *9*, 618.
11. (a) Beaulieu, P. L.; Tsantrizos, Y. S. *Curr. Opin. Invest. Drugs* **2004**, *5*, 838; (b) Rigat, K.; Wang, Y.; Hudyma, T. W.; Ding, M.; Zheng, X.; Gentles, R. G.; Beno, R. B.; Gao, M.; Roberts, S. B. *Antiviral Res.* **2010**, *88*, 197.
12. Erhardt, A.; Deterding, K.; Benhamou, Y.; Reiser, M.; Forns, X.; Pol, S.; Calleja, J. L.; Ross, S.; Spangenberg, H. C.; Garcia-Samaniego, J.; Fuchs, M.; Enriquez, J.; Wiegand, J.; Stern, J.; Wu, K.; Kukolj, G.; Marquis, M.; Beaulieu, P.; Nehmiz, G.; Steffgen, J. *Antivir. Ther.* **2009**, *14*, 23.
13. Glunz, P.W., et al. U.S. Patent 7112,501 B2, 2006, Biological enzyme assay protocol may also be found in Supplementary data.
14. (a) O'Boyle, D. R., II; Nower, P. T.; Lemm, J. A.; Valera, L.; Jun, J.-H.; Rigat, K.; Colonno, R.; Gao, M. *Antimicrob. Agents Chemother.* **2005**, *49*, 1346; (b) Fridell, R. A.; Qiu, D.; Wang, C.; Valera, L.; Gao, M. *Antimicrob. Agents Chemother.* **2010**, *54*, 3641.
15. Fossey, C.; Vu, A.-H.; Vidu, A.; Zarafu, I.; Laduree, D.; Schmidt, S.; Laumond, G.; Aubertin, A. *J. Enzyme Inhib.* **2007**, *22*, 591.
16. Procedure in Supplementary data.
17. Di Marco, S. et al *J. Biol. Chem.* **2005**, *280*, 29765.
18. Optimized models for compounds **2**–**4** in which the ether substituents were replaced with hydrogen atoms are shown superimposed with B. Coordinates for the model of B and ARG503 were extracted directly from the PDB entry (2BRK) for the NS5B/A complex. Superpositions were performed via RMS fitting **2**–**4** to B. All non-hydrogen atoms in the cyclohexyl and pendant phenyl rings and the central five-membered ring to which they are connected were used for the RMS fitting procedure. The color of carbon atoms in each molecule corresponds to that of the entry for that molecule in the inset table. Image created with Maestro™.
19. Schrodinger, *Maestro v 8.5*. Schrodinger: LLC, New York, NY, 2009.
20. Becke, A. D. *J. Chem. Phys.* **1993**, *98*, 5648.
21. Hehre, W. J.; Radom, L.; Schleyer, P. v. R.; Pople, J. A. *Ab Initio Molecular Orbital Theory*; John Wiley & Sons: New York, NY, 1986.
22. Lee, C.; Yang, W.; Parr, R. G. *Phys. Rev. B: Condens. Matter* **1988**, *37*, 785.
23. Parr, R. G.; Yang, W. Density–functional theory of atoms and molecules In *The International Series of Monographs on Chemistry*; Breslow, R., Goodenough, J. B., Halpern, J., Rowlinson, J. S., Eds.; Oxford University Press: New York, NY, 1989; Vol. 16,.
24. Q-Chem, version 3.1; Q-Chem, Inc: Pittsburgh, PA, 2007.
25. Johnson, F.; Malhotra, S. *J. Am. Chem. Soc.* **1965**, *87*, 5492.
26. (a) Harper, S. et al *J. Med. Chem.* **2005**, *48*, 1314; (b) Harper, S. et al *J. Med. Chem.* **2005**, *48*, 4547; (c) Beaulieu, P. L.; Jolicoeur, E.; Gillard, J.; Brochu, C.; Coulombe, R.; Dansereau, N.; Duan, J.; Garneau, M.; Jakalian, A.; Kuhn, P.; Lagace, L.; LaPlante, S.; McKercher, G.; Perrault, S.; Poirier, M.; Poupart, M.-A.; Stammers, T.; Thauvette, L.; Thavonekhham, B.; Kukolj, G. *Bioorg. Med. Chem. Lett.* **2010**, *20*, 857; (d) Narjes, F.; Crescenzi, B.; Ferrara, M.; Habermann, J.; Colarusso, S.; Ferreira, M.; Stansfield, I.; Mackay, A. C.; Conte, I.; Ercolani, C.; Zaramella, S.; Palumbi, M.-C.; Meuleman, P.; Leroux-Roles, G.; Giuliano, C.; Fiore, F.; De Francesco, R.; Rowley, M. *J. Med. Chem.* **2011**, *54*, 289.